ARTICLE

Zebrafish Ciliopathy Screen Plus Human Mutational Analysis Identifies *C21orf59* and *CCDC65* Defects as Causing Primary Ciliary Dyskinesia

Christina Austin-Tse,[1,2,20] Jan Halbritter,[3,20] Maimoona A. Zariwala,[4,20] Renée M. Gilberti,[5] Heon Yung Gee,[3] Nathan Hellman,[1] Narendra Pathak,[1] Yan Liu,[1] Jennifer R. Panizzi,[1] Ramila S. Patel-King,[5] Douglas Tritschler,[6] Raqual Bower,[6] Eileen O'Toole,[7] Jonathan D. Porath,[3] Toby W. Hurd,[8] Moumita Chaki,[8] Katrina A. Diaz,[8] Stefan Kohl,[3] Svjetlana Lovric,[3] Daw-Yang Hwang,[3] Daniela A. Braun,[3] Markus Schueler,[3] Rannar Airik,[3] Edgar A. Otto,[8] Margaret W. Leigh,[9] Peadar G. Noone,[9] Johnny L. Carson,[9] Stephanie D. Davis,[9] Jessica E. Pittman,[9] Thomas W. Ferkol,[10] Jeffry J. Atkinson,[11] Kenneth N. Olivier,[12] Scott D. Sagel,[13] Sharon D. Dell,[14] Margaret Rosenfeld,[15] Carlos E. Milla,[16] Niki T. Loges,[17] Heymut Omran,[17] Mary E. Porter,[6,21] Stephen M. King,[5,21] Michael R. Knowles,[18,21] Iain A. Drummond,[1,2,21,*] and Friedhelm Hildebrandt[3,19,21,*]

Primary ciliary dyskinesia (PCD) is caused when defects of motile cilia lead to chronic airway infections, male infertility, and situs abnormalities. Multiple causative PCD mutations account for only 65% of cases, suggesting that many genes essential for cilia function remain to be discovered. By using zebrafish morpholino knockdown of PCD candidate genes as an in vivo screening platform, we identified *c21orf59*, *ccdc65*, and *c15orf26* as critical for cilia motility. *c21orf59* and *c15orf26* knockdown in zebrafish and planaria blocked outer dynein arm assembly, and *ccdc65* knockdown altered cilia beat pattern. Biochemical analysis in *Chlamydomonas* revealed that the C21orf59 ortholog FBB18 is a flagellar matrix protein that accumulates specifically when cilia motility is impaired. The *Chlamydomonas ida6* mutant identifies CCDC65/FAP250 as an essential component of the nexin-dynein regulatory complex. Analysis of 295 individuals with PCD identified recessive truncating mutations of *C21orf59* in four families and *CCDC65* in two families. Similar to findings in zebrafish and planaria, mutations in *C21orf59* caused loss of both outer and inner dynein arm components. Our results characterize two genes associated with PCD-causing mutations and elucidate two distinct mechanisms critical for motile cilia function: dynein arm assembly for C21orf59 and assembly of the nexin-dynein regulatory complex for CCDC65.

Introduction

Apical cilia are essential cellular organelles that regulate embryonic development and organ function.[1] Cilia are microtubule-based structures projecting from the apical surface of nearly all cell types.[2] Embryonic cells employ nonmotile cilia to anchor membrane receptors and process signals from morphogens and to generate and respond to mechanical signals in the form of fluid flow and shear force in confined spaces.[1] Motile cilia and flagella propel germ cells through fluid environments and motile cilia on epithelial cells drive mucociliary clearance and create flow within fluid-filled lumens.[3] A wide spectrum of human pathologies, collectively termed ciliopathies, is associated with mutations in genes required for cilia function and includes Meckel-Gruber syndrome (MKS [MIM 249000]), nephronophthisis (NPHP [MIM 256100]), Bardet-Biedl syndrome (BBS [MIM 209900]), Joubert syndrome (JS [MIM 213300]), Senior-Løken syndrome (SLSN [MIM 266900]), Leber congenital amaurosis (LCA [MIM 204000]), polycystic kidney disease (PKD [MIM 173900]), oral-facial-digital syndrome (OFD [MIM 311200]), and cranioectodermal dysplasia (CED [MIM 614068]).[4–7] Clinical features of these syndromes include cystic kidney, organ laterality defects, nervous system development defects, and retinal degeneration, highlighting the ubiquity of cilia

[1]Nephrology Division, Massachusetts General Hospital, Charlestown, MA 02129, USA; [2]Division of Nephrology, Department of Genetics, Boston Children's Hospital, Harvard Medical School, Boston, MA 02115, USA; [3]Department of Medicine, Boston Children's Hospital, Harvard Medical School, Boston, MA 02115, USA; [4]Department of Pathology and Laboratory Medicine, University of North Carolina, Chapel Hill, NC 27599, USA; [5]Department of Molecular, Microbial and Structural Biology, University of Connecticut Health Center, Farmington, CT 06030, USA; [6]Department of Genetics, Cell Biology and Development, University of Minnesota, Minneapolis, MN 55455, USA; [7]The Boulder Laboratory for 3-D Electron Microscopy of Cells, Department of Molecular, Cellular, and Developmental Biology, University of Colorado, Boulder, CO 80309, USA; [8]Department of Pediatrics, University of Michigan, Ann Arbor, MI 48109, USA; [9]Department of Pediatrics, University of North Carolina School of Medicine, Chapel Hill, NC 27599, USA; [10]Department of Pediatrics, Washington University School of Medicine, St. Louis, MO 63110, USA; [11]Division of Pulmonary and Critical Care, Washington University School of Medicine, St. Louis, MO 63110, USA; [12]Laboratory of Clinical Infectious Diseases, National Institute of Allergy and Infectious Diseases, National Institutes of Health, Bethesda, MD 20892, USA; [13]Department of Pediatrics, University of Colorado School of Medicine, Aurora, CO 80045, USA; [14]Department of Pediatrics, The Hospital for Sick Children, University of Toronto, Toronto, ON M5G 1X8, Canada; [15]Children's Hospital and University of Washington, Seattle, WA 98105, USA; [16]Department of Pediatrics, Stanford University, Stanford, CA 94304, USA; [17]Department of General Pediatrics, University Children's Hospital Muenster; 48149 Muenster, Germany; [18]Cystic Fibrosis/Pulmonary Research and Treatment Center, Chapel Hill, NC 27599, USA; [19]Howard Hughes Medical Institute, Chevy Chase, MD 20815, USA
[20]These authors contributed equally to this work
[21]These authors contributed equally to this work and are co-senior authors
*Correspondence: idrummond@partners.org (I.A.D.), friedhelm.hildebrandt@childrens.harvard.edu (F.H.)
http://dx.doi.org/10.1016/j.ajhg.2013.08.015. ©2013 by The American Society of Human Genetics. All rights reserved.

function.[4] Mutations disrupting cilia motility in humans cause primary ciliary dyskinesia (PCD, CILD [MIM 244400]), which has an estimated incidence of 1 in 16,000 to 20,000 live births.[8] Affected individuals present with sterility, organ laterality defects, hydrocephalus, chronic upper and lower respiratory tract infections, and otitis media. Twenty-one genes harboring PCD-causing mutations have been identified by a combination of traditional genetic mapping and selective screening of cilia motility genes identified in model systems such as *Chlamydomonas reinhardtii* and *Danio rerio* (Table S2).[8]

Motile cilia require outer dynein arms (ODAs) and inner dynein arms (IDAs) to achieve proper waveform. Mutations in genes encoding the structural elements of dynein arms or cytoplasmic components required for arm preassembly and transport result in loss of ODAs and IDAs with subsequent cilia paralysis.[9–12] Cilia dysmotility can also arise from mutations in genes encoding one of two complexes required for the coordination of dynein arm activity: the N-DRC and the radial spoke complex (RS).[13–16] The N-DRC generates resistance to microtubule sliding, and this resistance contributes to optimal alignment of microtubule doublets for productive flagellar motility.[17] Recently, mutations in *DRC1/CCDC164* (MIM 615288) and *DRC4* were shown to impair N-DRC function,[14,17] although the function of other N-DRC proteins remains to be determined.

More than one-third of PCD cases remain genetically uncharacterized and have yet to be linked to mutations in known genes.[8] At the same time, informatic and proteomic analyses of cilia have identified more than 1,000 cilia-associated proteins and genes that might harbor mutations in affected individuals.[18] To identify cilia proteome genes associated with yet-uncharacterized PCD mutations, we screened for ciliopathy phenotypes in zebrafish after morpholino-induced knockdown of genes encoding proteins present in multiple cilia proteomes and highly expressed in ciliated tissues. We focused further on three genes that when knocked down produced robust ciliopathy phenotypes resulting from defects in cilia motility. We show that two of these genes, *C21orf59* and *CCDC65* (MIM 611088), are mutated in human PCD, validating this strategy for identifying human disease mutations.

Material and Methods

Zebrafish Strains and Maintenance

TU-AB and *Tg(ubiquitin:arl13b-GFP)* zebrafish lines were maintained according to standard procedures.[19] All embryos were raised in E3 egg water. Embryos analyzed at 24 hpf were treated with phenylthiourea (PTU) so that pigment would not develop. The *Tg(ubiquitin:arl13b-GFP)* fish line was generated by a standard Tol2-mediated transposition approach.[20] The vector for transgenesis was generated by multisite Gateway recombination of the following vectors: pDONR221 containing the zebrafish *arl13b* coding sequence (from Zhaoxia Sun), p5E containing the ubiquitin promoter (from Leonard Zon), p3E-EGFPpA, and pDESTTol2CG2, both from the Tol2 kit.[21]

In Situ Hybridization

For some of the candidates assessed in the morpholino screen, expression data were available from a large-scale in situ hybridization screen.[22] We generated digoxygenin-labeled antisense RNA probes for zebrafish *c21orf59*, *ccdc65*, *c15orf26*, *ccdc63*, and *enkurin/c10orf63* by in vitro transcription from EST clones purchased from Open Biosystems of Thermo Scientific. Whole-mount in situ hybridization was performed as previously described.[23] Stained embryos were cleared with dimethyl formamide and imaged on a Leica MZ12 stereomicroscope with a Spot Image digital camera.

Morpholino Injections

Foxj1a knockdown was achieved with previously described morpholinos.[23] For the morpholino screen, the morpholinos listed in Table S1 (available online) were diluted to 0.25 mM and 0.5 mM concentrations in 1× injection solution containing 100 mM KCl, 10 mM HEPES, and 0.1% phenol red. TU-AB embryos were injected with 4.6 nl diluted morpholino injection mixes in the yolk at the 1–4 cell stage and allowed to develop at 28°C. At 24 hpf, injected clutches were screened for dead embryos and embryos displaying significant neural cell death. When these phenotypes were observed in >30% of the clutch, the morpholino dose was considered to be toxic, and embryos were not included in further analyses. Remaining embryos were incubated from 33 to 48 hpf in a low dose of pronase enzyme so that chorions would be removed. At 48 hpf, axis curvature, otolith number, and hydrocephalus phenotypes were assessed. The presence of pronephric cysts was scored at 60 hpf.

RT-PCR

To assess splicing defects caused by morpholino injection, we extracted RNA from pools of five embryos per condition by using TRI reagent (Molecular Research Center). cDNA was synthesized with gene-specific primers and Superscript II reverse transcriptase (Invitrogen). We then used primers binding in exons adjacent to the morpholino binding site (Table S2) in nested PCR to amplify wild-type and morphant products. PCR products were separated on agarose gels, and wild-type and morphant bands were extracted for sequencing. Products from PCR1 were used as templates for PCR2.

In Vivo Imaging of Zebrafish Cilia

Olfactory placode and pronephric duct cilia motility defects were assessed at 48 hpf by high-speed video microscopy. For imaging, embryos were anesthetized in 0.2 mg/ml tricaine and immobilized in 3% methylcellulose. Movies were acquired at 240 frames per second by a high-speed Dragonfly Express video camera (Point Gray Research) and converted to 15 frames per second for visualization of beat rate and amplitude. Kymograms were generated with the line scan function in ImageJ. For imaging of live Kupffer's vesicle (KV) cilia, *Tg(ubiquitin:arl13b-GFP)* fish were embedded in 3% low-melt agarose at the 7–12 somite stage. Z stacks of the entire vesicle were acquired on a Zeiss LSM5 Pascal confocal microscope. The percentage of motile cilia per KV was scored on the basis of cilia appearance (zig zags versus straight lines) in acquired z series.

Immunoblots

Immunoblotting on 24 hpf zebrafish embryo extracts was performed as previously described[24] with mouse anti-human

C21orf59 (1:500, Santa Cruz) or mouse anti-α-tubulin B512 (Sigma 1:5,000) and a peroxidase-conjugated goat anti-mouse secondary antibody (Jackson Immunoresearch, 1:10,000).

Immunofluorescence

For staining of zebrafish pronephric cilia, 2 dpf wild-type and morphant embryos were fixed in Dents fixative (80% MeOH, 20% DMSO) overnight at 4°C. Embryos were transferred to 100% MeOH and incubated for 1 hr at room temperature prior to rehydration through a MeOH gradient. Samples were blocked for 2 hr at room temperature in PBST + 10% normal goat serum (NGS) prior to incubation in primary antibodies at 4°C overnight. Primary antibodies were diluted in blocking buffer as follows: rabbit anti-IFT88 (1:400, gift from Brain Perkins), 6-11B-1 anti-acetylated α-tubulin (1:400, Sigma), and GTU88 anti-γ-tubulin (1:400, Sigma). After PBST washes, embryos were incubated overnight in a 1:800 dilution of Alexa 488- or 546-conjugated goat anti-rabbit or goat anti-mouse secondary antibodies (Invitrogen). For double staining by two mouse antibodies, a modified immunostaining protocol was performed as previously described.[25] For imaging, stained embryos were equilibrated in clearing solution (53% benzyl alcohol, 45% glycerol, 2% N-propyl gallate), and two-color z series were acquired on a Zeiss LSM5 Pascal confocal microscope via sequential laser excitation.

Immunofluorescence of Human Respiratory Epithelium

Cells were treated with 4% paraformaldehyde, 0.2% Triton X-100, and 1% skim milk (all percentages are v/v) before incubation with primary (2–3 hr at room temperature or overnight at 4°C) and secondary (25 min at room temperature) antibodies. Appropriate controls were performed omitting the primary antibodies. Anti-acetylated tubulin was used at a 1:10,000 dilution, and rabbit polyclonal anti-a/b-tubulin was used at a 1:300 dilution (#2148; Cell Signaling). Mouse monoclonal anti-DNAH5 and rabbit polyclonal anti-DNALI1 antibodies were generated as reported.[11,26] Highly cross-adsorbed secondary antibodies goat anti-mouse Alexa Fluor 488 (1:1,000; A11029) and goat anti-rabbit Alexa Fluor 546 (1:1,000; A11035) were from Molecular Probes (Invitrogen). DNA was stained with Hoechst33342 (1:1,000; 14533-100MG, Sigma). Immunofluorescence images were taken with a Zeiss Apotome Axiovert 200 microscope and processed with AxioVision 4.8 and Adobe Creative Suite 4.

Electron Microscopy

D. rerio, *S. mediterranea*, and human biopsy samples were fixed and prepared for transmission electron microscopy (TEM) as previously described.[27–29] *S. mediterranea* was prepared for scanning electron microscopy (SEM) as previously described.[29]

Zebrafish mRNA Rescue

Full-length human *C21orf59* and *CCDC65* coding domains were cloned into the pDONR221 plasmid (Invitrogen) and subcloned into the pCSmCherryDest expression vector[21] via Gateway technology (Invitrogen). For mutation analysis, the pCSmCherryDest-*hsC21orf59* construct was mutagenized with a standard PCR-based site-directed mutagenesis approach.[30] Capped RNAs were synthesized from linearized vectors with the SP6 mMessage mMachine kit (Invitrogen). RNA products were column purified with the RNeasy Mini Kit (QIAGEN) prior to injection at 25–400 pg doses into 1 cell stage zebrafish embryos. For rescue of morphant phenotypes, morpholinos were injected into 2–4 cell embryos that had previously been injected with RNA.

Schmidtea mediterranea

Planarians were acquired and maintained according to previously described methods.[29] For generation of the RNAi vectors, part of the FBB18 coding sequence was cloned into the L4440 vector.[31] RNAi knockdown and confirmatory RT-PCR were conducted according to standard protocols.[32,33] For gliding assays, planarians were placed in petri dishes, and animal movement was recorded with a color CCD camera (DFK 31BU03; The Imaging Source). The distance traveled by each planarian was measured directly from the video. Movies were decompiled, cropped, combined, and labeled with Blaze Media Pro, VirtualDub, and ImageJ.

Chlamydomonas reinhardtii

All strains were obtained from the *Chlamydomonas* center and were raised according to standard protocols.[34] For examination of flagellar protein content in Figure 2, cells were harvested by centrifugation and deflagellated by dibucaine treatment. Flagella were isolated by previously described methods. Proteins were separated on 10% SDS gels and either stained with Coomassie brilliant blue or blotted to nitrocellulose and probed with antibodies. Primary antibodies used were anti-*D. rerio* C21orf59/FBB18 (raised against multiple synthetic peptides distributed throughout the protein sequence; AbMart) and anti-D1blC.[35]

FAP250/*ida6* Cloning

An ~9.5 kb genomic fragment encoding FAP250 was subcloned from BAC 31n21 with DraI and SpeI. The FAP250 subclone was linearized with NotI and cotransformed into *ida6* along with the plasmid pSI103 containing the selectable marker *aphVIII*.[36] Transformants were selected on Tris-acetate-phosphate medium containing 10 μg/ml paromomycin and screened for improved motility by phase-contrast microscopy as described previously.[17] The *ida6* mutation was identified by the direct sequencing of PCR products obtained from wild-type and *ida6* genomic DNA via primers spanning 500–1,000 bp regions across the *FAP250* transcription unit. An RNA blot containing total wild-type RNA isolated from cells before (0 min) and 45 min after deflagellation was probed with an ~1.3 kb RT-PCR product obtained from wild-type cDNA by the forward primer 5′-CCGCAAGGACGCCAT TATG-3′ and the reverse primer 5′-TGTTCCGCTCCGTGA GTGTG-3′. For Figure 3, isolated axonemes were prepared and subjected to immunoblot analysis with antibodies against FAP250, RSP16, and tektin. Alternatively, axonemes were fixed for electron microscopy, and computer image averaging was performed as described.[17,37]

Research Subjects

We obtained blood samples and pedigrees after receiving informed consent from individuals with PCD and their family members. Approval for research on human subjects was obtained from the institutional review boards of the universities of North Carolina, Michigan, Freiburg, and Münster, the Boston Children's Hospital, and the other institutions involved. The diagnosis of PCD was based on published clinical criteria, including compatible clinical phenotype, hallmark diagnostic defects in ciliary ultrastructure, and low nasal nitric oxide (nNO).[38] Genomic DNA was isolated by standard methods from blood samples or from lymphocyte cultures after Epstein-Barr virus transformation.

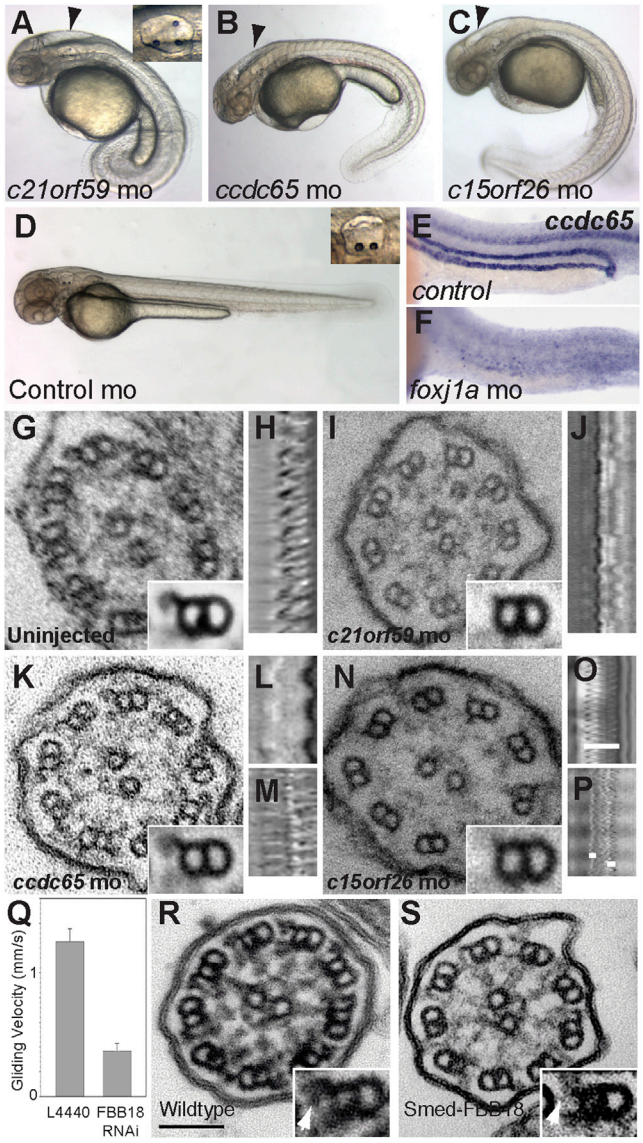

Figure 1. Zebrafish Knockdown Screen Identifies *c21orf59*, *ccdc65*, and *c15orf26* as Essential for Cilia Motility

(A–D) Morpholino knockdown of *c21orf59* (A), *ccdc65* (B), and *c15orf26* (C) produces ciliopathy phenotypes in zebrafish, including axis curvature, hydrocephalus (arrowheads), and supernumerary otoliths (insets in A and D). Phenotypes are not observed in control injected embryos (D).

(E and F) Expression of *ccdc65* mRNA in ciliated tissues, visible in control (E), is eliminated by *foxj1a* morpholino knockdown (F).

(G) Ultrastructure of wild-type cilia shows the 9+2 arrangement of microtubules with inner and outer dynein arms projecting from the A subfibers of each doublet in cross sections and averaged doublets (inset; n = 75).

(H) Kymogram of wild-type olfactory cilia beat from high-speed microvideo (Movie S1) shows rhythmic cilia wave form at 31 Hz.

(I) *c21orf59* morphant cilia ultrastructure showing loss of dynein outer arm motor domains in computer-averaged microtubule doublets (inset; n = 30 doublets).

(J) Kymogram of *c21orf59* morphant olfactory cilia beat (Movie S3) shows near-complete cilia paralysis.

(K) *ccdc65* morphant cilia show normal dynein arm ultrastructure in averaged doublets (inset; n = 27).

(L and M) Kymograms of *ccdc65* morphant olfactory cilia beat shows either complete cilia paralysis (L; Movie S4) or dyskinetic, faster beat rate (48 Hz; M; Movie S5).

(N) Similar to *c21orf59*, outer dynein arms are lost in *c15orf26* morphants (inset; n = 8).

(O) Kymogram of control pronephric cilia (Movie S2) shows a beat rate of 66 Hz and a wave amplitude of 8.6 μm (white bar in O).

(P) Kymogram of *c15orf26* morphant pronephric cilia (Movie S6) shows severely reduced beat amplitude (white bars = 1.8 μm) or paralysis.

(Q–S) RNAi knockdown of the *c21orf59* ortholog in planaria, *FBB18*.

(Q) *Smed-FBB18* (*RNAi*) significantly reduces cilia-driven gliding locomotion of planaria (Movie S7).

(R and S) Ultrastructure of control (R) and *Smed-FBB18* (*RNAi*) (S) cilia. Insets show defects in *Smed-FBB18* (*RNAi*) ODA assembly (arrows). The scale bar represents 100 nm.

Mutation Analysis

Mutation analysis in candidate genes was performed with a barcoded, high-throughput exon-sequencing technique that we recently developed.[39] Segregation analysis was done by Sanger dideoxy-terminator resequencing for confirmation and segregation of potential disease-causing variants in the respective affected individuals, their affected siblings, and their parents. Sequencing was performed with BigDye Terminator v3.1 Cycle Sequencing Kit on an ABI 3730 XL sequencer (Applied Biosystems). Sequence traces were analyzed with Sequencher (v.4.8) software (Gene Codes Corporation). Polymerase chain reaction (PCR) was performed by a touchdown protocol described previously.[40] At the University of North Carolina, we used Sanger sequencing with an ABI 3130XL and analysis with Sequencher. At Universitaetsklinik Muenster, Sanger sequencing was performed with an Applied Biosystems 3730xl DNA Analyzer, and data were analyzed with the CodonCode software provided by CodonCode Corporation.

Results

A Functional Screen of Cilia Proteome Genes in Zebrafish and Planaria

To characterize the function of genes not previously linked to PCD, we screened a set of uncharacterized genes encoding proteins present in multiple cilia proteomes[41–50] by knockdown in zebrafish (Table S3). Knockdown of three genes, *c21orf59/FBB18* (RefSeq accession number NM_200088.1), *ccdc65/FAP250* (RefSeq NM_001002603.2), and *c15orf26* (RefSeq NM_001017774.1) resulted in strong ciliopathy phenotypes, including those involving pronephric cysts, axis curvature, left-right asymmetry defects, and hydrocephalus (Figures 1A–1D and S1), suggesting that these genes play essential roles in cilia function. Immunostaining via antibodies against acetylated-tubulin (axonemes), γ-tubulin (basal bodies), and Ift88 (intraflagellar transport particles) did not detect structural cilia abnormalities (Figure S2), suggesting that ciliopathy phenotypes might be due to altered cilia motility. Consistent with other essential motile cilia genes,[23,51] *c21orf59*, *ccdc65*, and *c15orf26* mRNA expression was dependent on the transcriptional regulator Foxj1a (Figures 1E, 1F, and S3). Live imaging of olfactory placode and pronephric cilia by high-speed video microscopy revealed that compared to controls (Movies S1 and S2; Figures 1H and 1O), cilia in *c21orf59*, *ccdc65*, and

c15orf26 morphants were either paralyzed or dyskinetic (Movies S3, S4, S5, and S6; Figures 1J, 1L, 1M, and 1P). Cilia ultrastructure analysis revealed that outer dynein arms were missing in *c21orf59* and *c15orf26* morphants but not in *ccdc65* morphants, indicating that these genes control cilia motility by distinct mechanisms (Figures 1G, 1I, 1K, and 1N; insets).

Ventral cilia in the planarian *Schmidtea mediterranea* generate a synchronized beating pattern used for locomotion.[29] Consistent with previously published planarian motility mutants,[29] complete knockdown of planaria *c21orf59/fbb18* (mk4.000443.01.01)[52] (Figure S4) significantly reduced cilia-driven gliding motion (Figure 1K; Movie S7). Ventral cilia were normal in number and length (Figure S4) but showed defects in assembly of outer dynein arms; these results are similar to those from zebrafish *c21orf59* knockdown (Figures 1L and 1M), suggesting that the requirement for C21orf59 in cilia motility is well conserved.

Mutations in *C21orf59* Cause Human Primary Ciliary Dyskinesia

To investigate whether *C21orf59* mutations occur in humans with PCD, we examined a worldwide cohort of 295 individuals with PCD by targeted exon resequencing of all seven exons of *C21orf59* (RefSeq accession number NM_021254.2) by a bar-coded, high-throughput exon-resequencing technique.[39] All screened individuals suffered from recurrent bronchitis, sinusitis, and/or otitis media. Situs inversus (Figure 2A) and situs ambiguous were present in 112 and 26 individuals, respectively. Ultrastructural analysis of nasal brushings revealed that 85 affected individuals showed defective or missing outer dynein arms, 45 showed defective or missing outer and inner dynein arms, 53 showed defective inner dynein arms with microtubular disorganization, and nine showed central apparatus defects. In the remaining individuals, PCD was ascertained on the basis of clinical phenotype, the presence of situs abnormalities, and low levels of nasal nitric oxide. In total, we identified disease-causing *C21orf59* mutations in four out of 295 families with PCD (A4204 [#46], A5014_087 [#143], A5014_384 [#508], 5014_513 [#652]) with 3 different truncating mutations: c.292C>T (p.Arg98*), c.735C>G (p.Tyr245*), and c.792_795delTTTA (p.Tyr264*) (Table 1; Figures 2B–2E). One of the mutations (c.735C>G) was putatively homozygous in three unrelated families, two of which had known Ashkenazi Jewish ethnicity (Table 1; Figure 2E). Further analysis of all three affected individuals by the use of 20 SNP markers ~2 Mb up and downstream of the c.735C>G mutation revealed that this mutation is located within a shared haplotype of ~1 Mb (Figure S5). This result strongly indicates the presence of a founder effect involving a common distant ancestor for all three families. Because parental DNA for segregation analysis was not available in family A5014_087, we cannot rule out hemizygosity in this affected individual. However, if hemizygosity rather than homozygosity were present, that would not alter the assumption of the absence of a normal allele in the affected individual and thereby would not affect our conclusions. Given the parental segregation in the other two families, carrying the same mutation and its supposed founder effect, homozygosity is nevertheless most likely to be present in all three families. For exclusion of known genetic causes of PCD, 19 known genes previously linked to PCD were screened in all four families with *C21orf59* mutations, but no explanatory mutations were detected (Table S4). In addition to truncating mutations, single heterozygous *C21orf59* missense variants were found in three individuals without identification of a second mutated allele: c.97C>T (p.Arg33Trp), c.422A>G (p.Asp141Gly), and c.517G>T (p.Asp173Thr). Phenotypically, these individuals presented with low nasal nitric oxide, sinus disease, otitis media, and/or bronchiectasis but normal ciliary ultrastructure, suggesting that these mutations might be either hypomorphic or not causative of PCD.

Human C21orf59 is a 290 aa protein that contains a coiled-coil (CC) and a domain of unknown function (DUF2870) at the C-terminal end, as does its zebrafish homolog (90% similarity, 73% identity) (Figures 2F, 2G, and S6). The identified human mutations would be predicted to encode truncated proteins that lack either the last 193 (p.Arg98*), 45 (p.Tyr245*), or 26 (p.Tyr264*) amino acids (Figures 2D–2G). Alternatively, these mutant mRNAs might be subject to nonsense-mediated mRNA decay (see below). Cilia ultrastructure of all affected individuals carrying mutations in *C21orf59* showed an absence of both outer- and inner-dynein-arm components (Figure 2B). To confirm the absence of both outer- and inner-dynein-arm components in *C21orf59* mutant cilia, we obtained nasal brushing respiratory epithelial cells from individual A5014_087-21 carrying the c.735C>G (p.Tyr245*) mutation (Table 1) and immunostained the cells with antibodies specific to DNAH5 (ODAs) and DNALI1 (IDAs). Both DNAH5 (Figure 2H) and DNALI1 (Figure 2I) were absent from *C21orf59* mutant cilia, confirming the absence of both outer and DNALI1-related inner arms. Consistent with results for zebrafish and planaria *c21orf59/fbb18*-deficient cilia, live imaging of *C21orf59* mutant cilia in human nasal epithelia revealed complete paralysis (Movie S8).

To test the pathogenicity of the identified mutations, we injected synthetic mRNA containing *C21orf59* missense variants c.97C>T (p.Arg33Trp), c.422A>G (p.Asp141Gly), or c.517G>T (p.Asp173Thr) or the most C-terminal truncating mutation, c.792_795delTTTA (p.Tyr264*) into zebrafish *c21orf59* morphants and assayed KV cilia motility (Figure 3). C21orf59-deficient zebrafish have paralyzed KV cilia (Figures 3A–3C) and abnormal heart looping (Figure 3D). Injection of wild-type human *C21orf59* mRNA rescued morphant KV cilia motility (Figure 3C) and heart looping (Figure 3D). In contrast, c.792_795delTTTA (p.Tyr264*) mutant RNA injection failed to rescue cilia motility or heart looping (Figures 3C and 3D).

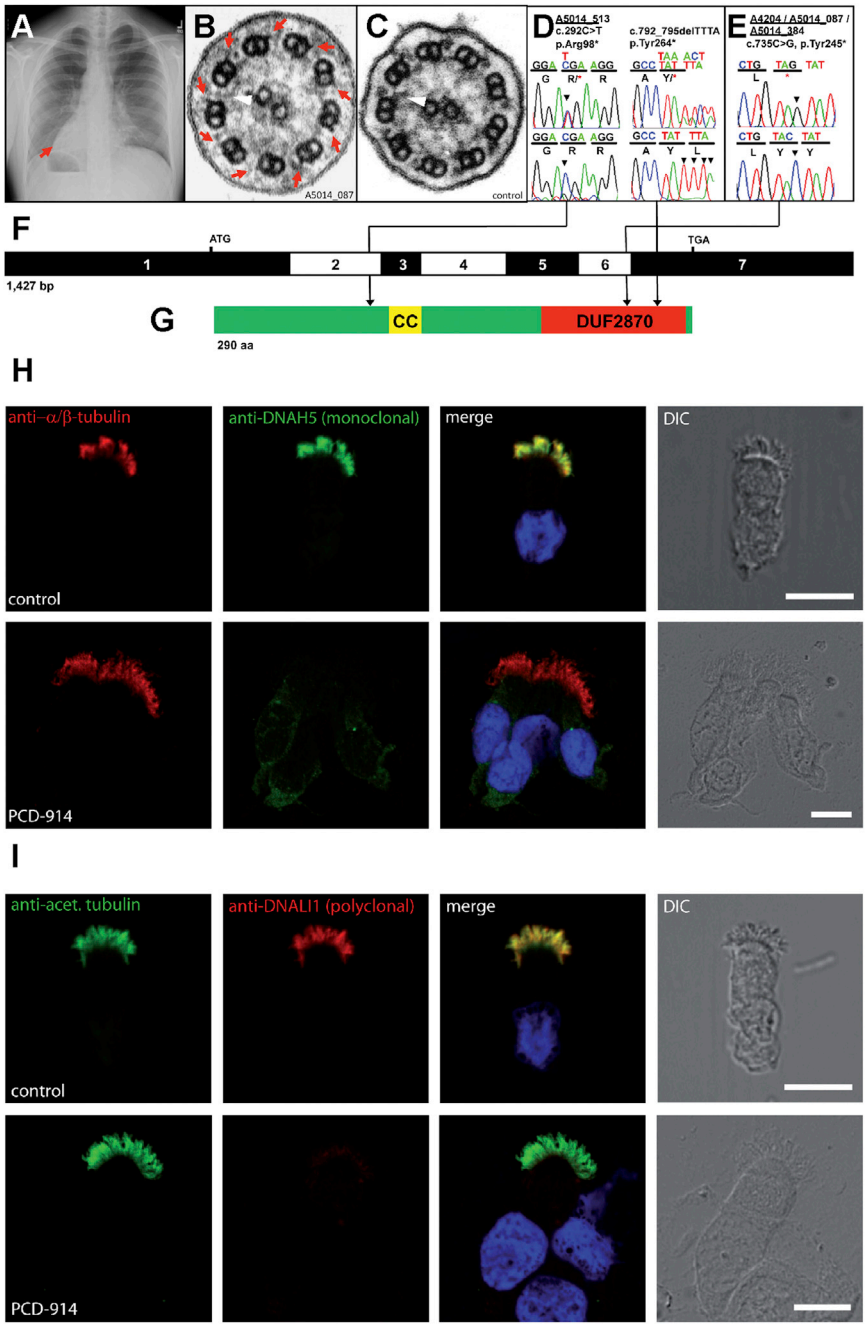

Figure 2. Identification of Recessive Mutations in *C21orf59* in Four Families with Primary Ciliary Dyskinesia and Loss of Ciliary Dynein Arms in Individuals with PCD

(A) Chest X-ray of individual A5014_087-21, showing situs inversus. Red arrow indicates the apex of the heart on the right side.

(B and C) TEM of individual A5014_087-21 (B) showing shortened/missing outer (red arrows) and inner (white arrowheads) dynein arms compared to control cilia (C).

(D and E) Three different *C21orf59* mutations detected in four independent families with PCD. Family number (underlined), mutation (arrowhead), and predicted translational changes are indicated. For the mutations detected, arrows indicate positions in relation to exons. Sequence trace is shown for mutation above normal controls.

(F) Exon structure of human *C21orf59* cDNA. Positions of start codon (ATG) and stop codon (TGA) are indicated.

(G) C21orf59 protein putatively contains a coiled-coil (CC) and a domain of unknown function (DUF2870) at the C-terminal end.

(H and I) Immunolocalization of DNAH5 and DNALI1 in human respiratory epithelial cells from individual A5014_087-21 carrying the *C21orf59* c.735C>G (p.Tyr245*) mutation.

(H) Immunofluorescence analysis of human respiratory epithelial cells via specific antibodies directed against the outer dynein arm heavy chain DNAH5 (green). As a control, axoneme-specific antibodies against α/β-tubulin (red) were used. Nuclei were stained with Hoechst 33342 (blue). In respiratory epithelial cells from healthy probands, DNAH5 (green) localizes along the entire length of the axonemes. DNAH5 (green) absent from cilia in respiratory epithelial cells from individual A5014_087-21.

(I) Immunofluorescence analysis of human respiratory epithelial cells using specific antibodies directed against the inner dynein arm intermediate chain DNALI1 (red). As a control, axoneme-specific antibodies against acetylated α-tubulin (green) were used. Nuclei were stained with Hoechst 33342 (blue). DNALI1 is localized along the entire length of the axonemes of healthy probands. In contrast, in respiratory cells of individual A5014_087-21, DNALI1 is absent from cilia.

Scale bars in (H) and (I) represent 10 μm.

Of the missense variants, only the c.422A>G (p.Asp141Gly) variant showed reduced rescue (Figure 3C), indicating that these mutations are likely to be benign polymorphisms or, for c.422A>G, potentially a hypomorphic mutation. The p.Tyr264* protein lacking the last 26 amino acids was not stable in zebrafish embryos, even when mRNA was injected at concentrations up to 10-fold higher than the wild-type (Figure S7), suggesting that this protein may be rapidly degraded or that the mRNA may be subject to nonsense-mediated mRNA decay.

The *C. reinhardtii* C21orf59 Ortholog FBB18 Is a Flagellar Matrix Protein Regulated by Cilia Motility

Failure of ODA assembly in C21orf59/FBB18-deficient cilia suggested that C21orf59/FBB18 may act as an ODA structural component or be involved in trafficking and assembly of cilia dynein arms. Using a cross-reacting C21orf59/FBB18 antibody (Figure S8), we found that C21orf59/FBB18 (RefSeq accession number XM_001699148.1) localized exclusively to the flagellar matrix in wild-type and ODA mutant *C. reinhardtii* axonemes (Figure 4A), similar

Table 1. Mutations of *C21orf59* or *CCDC65* in Six Families with Primary Ciliary Dyskinesia

Family-Individual	Ethnic Origin (Sex)	Nucleotide Alteration (Segregation)	Deduced Protein Change	Exon/Intron (Zygosity)	nNO (nl/min)	Situs Inversus	TEM	Video Microscopy	Additional Clinical Presentation
C21orf59									
A4204 (#46)-21 (#274)	Brazilian (male)	c.735C>G[a] (P, het; M, het)	p.Tyr245*	6 (hom)	42.5	yes	ODA+IDA defects	immotile cilia	NRD, SD, BE
A5014_087 (#143)-21 (#914)	Ashkenazi Jewish (male)	c.735C>G[a] (P, ND; M, ND)	p.Tyr245*	6 (hom/hem)	8.9	yes	ODA+IDA defects	ND	NRD, OM, SD
A5014_384 (#508)-21 (#1637)	Ashkenazi Jewish (female)	c.735C>G[a] (P, ND; M, het)	p.Tyr245*	6 (hom/hem)	13.9	yes	ODA+IDA defects	ND	NRD, OM, SD, BE
A5014_513 (#652)-21 (#2003)	European-American (female)	c.292C>T[b] (P, WT; M, het), c.792_795delTTTA (P, het; M, WT)	p.Arg98*, p.Tyr264*	2 (het),7 (het)	15.7	no	partial ODA+IDA defects	ND	NRD, OM, SD
CCDC65									
A5014_493 (#629)-21 (#1929) and -22 (#2005)	Ashkenazi Jewish (male and male)	c.877_878delAT (P, ND; M, ND)	p.Ile293Profs*2	6 (hom and hem)	33.2 (-21) and ND (-22)	no	normal DA	dyskinetic cilia	OM, SD, BE (-21) and OM, BE (-22)
A5014_656 (#798) -21 (#2272)	Ashkenazi Jewish (female)	c.877_878delAT (P, het; M, het)	p.Ile293Profs*2	6 (hom)	20	no	normal DA+CA	dys-/ hyperkinetic cilia	NRD, OM, SD, BE

Abbreviations are as follows: BE, bronchiectasis; CA, central apparatus/central pair; DA, dynein arms; hom, homozygous; het, heterozygous; hem, hemizygous; M, maternal; nNO, nasal nitric oxide, normal range: 376 ± 124 nl/min (mean ± SD);[53] ODA, outer dynein arm; OM, otitis media; ND, no data; NRD, neonatal respiratory distress; P, paternal; SD, sinus disease or chronic sinusitis.
[a]Mutation is in 1000 Genomes database: rs202094637 (GG = 0/GC = 1/CC = 661).
[b]Mutation is in EVS (Exome variant server) database: rs143740376 (TT = 0/TC = 2/CC = 6501).

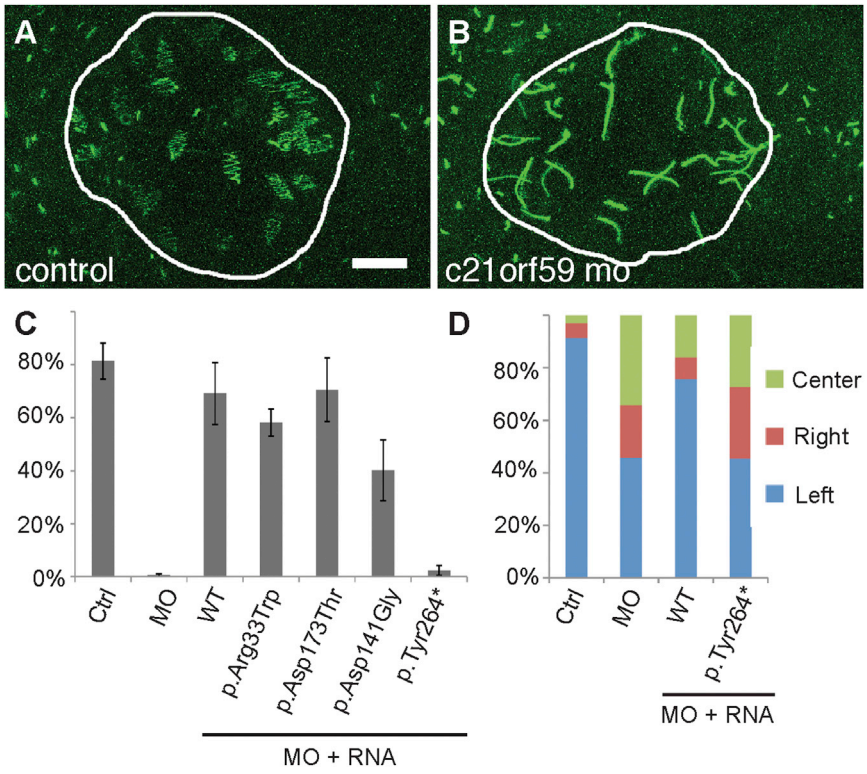

Figure 3. Functional Analysis of *C21orf59* Alleles in Zebrafish

(A and B) Control (A) or *c21orf59* (B) morpholinos were injected into the transgenic *Tg(ubiquitin:arl13b-GFP)* zebrafish line. Laser scanning confocal imaging reveals motile, GFP-positive Kupffer's vesicle cilia as "zigzags" (A). Cilia in *c21orf59* morphant KV's (B) were paralyzed and appear as straight lines. Scale bar represents 5 μm.

(C) Quantification of the percentage of motile cilia within KV. Coinjection of *c21orf59* morpholino with a full-length human *C21orf59* mRNA or three *C21orf59* missense alleles rescued the motility of KV cilia, whereas injection of human *C21orf59* mRNA bearing the c.792_795delTTTA (p.Tyr264*) mutation failed to rescue cilia motility. n = 3–6 embryos per sample, as indicated. Error bars indicate SEM.

(D) Injection of WT, but not c.792_795delTTTA (p.Tyr264*) mutant, *C21orf59* human mRNA rescued heart looping morphogenesis in zebrafish *c21orf59* morphants.

to the IFT particle. C21orf59/FBB18 protein levels were low in wild-type axonemes but, surprisingly, were dramatically elevated in flagella of motility-impaired mutants, but not in a mutant with close to wild-type cilia motility (*oda11*; Figure 4B). Increased abundance of C21orf59/FBB18 protein was also observed in cell bodies of motility-impaired mutants, suggesting that C21orf59/FBB18 protein is induced or stabilized when cilia motility is impaired (Figure 4C). Although associated with the flagellar matrix, C21orf59/FBB18 did not comigrate with IFT particle proteins in Superose 6 filtration (Figure 4D). Consistent with its dynamic pattern of flagellar association in *C. reinhardtii*, C21orf59/FBB18 protein was predominantly cytoplasmic in rat trachea (Figures 5A, 5B, and S9). In rat trachea, C21orf59/FBB18 partially colocalized with SAS6 in cytoplasmic puncta, suggesting a centrosomal localization (Figure 5B).

Mutations in *CCDC65* Cause Human Primary Ciliary Dyskinesia

To screen for human *CCDC65* (RefSeq NM_033124.4) mutations in individuals with PCD, we examined all eight *CCDC65* coding exons and exon-intron boundaries in our cohort of 295 individuals with PCD by applying the above-described high-throughput technique (Figures 6A–6F). We identified truncating mutations in three individuals from two families (Figure 6A) whose affected members shared the same putatively homozygous frameshift mutation, c.877_878delAT (p.Ile293Profs*2) (Table 1; Figures 6D–6F). Because parental DNA for family A5014_493 [#629] was not available, we cannot completely exclude hemizygosity in this case. Taken together with the segregation of family A5014_656 [#798], who shares not only the same mutation but also the same Ashkenazi Jewish ethnicity, a founder effect and thereby homozygosity of this mutation is very likely to be present in both families. In the affected individuals (A5014_493 [#629] -21, -22, and A5014_656 [#798]), cilia ultrastructure showed normal outer dynein arms, radial spokes, and central pairs but a reduction in inner dynein arms and nexin links (Figures 6B and 6C). Microtubule disorganization was also observed in 5%–15% of cilia cross sections (Figure 6B, inset), suggesting that the reduction in nexin links may lead to overall structural instability in a subset of PCD individual cilia. Live imaging of PCD individual nasal epithelial cilia revealed a stiff, dyskinetic cilia waveform (Movie S9), similar to that of zebrafish *ccdc65* morphant cilia (Movie S5). The affected individuals suffered from recurrent bronchitis, sinusitis, and/or otitis media. Situs abnormalities were not present in affected individuals, and fertility status could not be ascertained. Biallelic mutations in any of 19 genes previously linked to PCD were excluded by the same mutation-analysis approach (Table S4). The human CCDC65 protein shows a 69% similarity and 41% identity to its zebrafish homolog (Figure S10). CCDC65 comprises 484 amino acids and contains two coiled-coil domains, one of which is truncated by the identified frameshift mutation (Figures 6E, 6F, and S10).

The *CCDC65 C. reinhardtii* Ortholog *FAP250* Is an Essential Component of the Nexin-Dynein Regulatory Complex

Unlike C21orf59l/FBB18-deficient cilia, Ccdc65-deficient zebrafish and human cilia did not show ODA defects

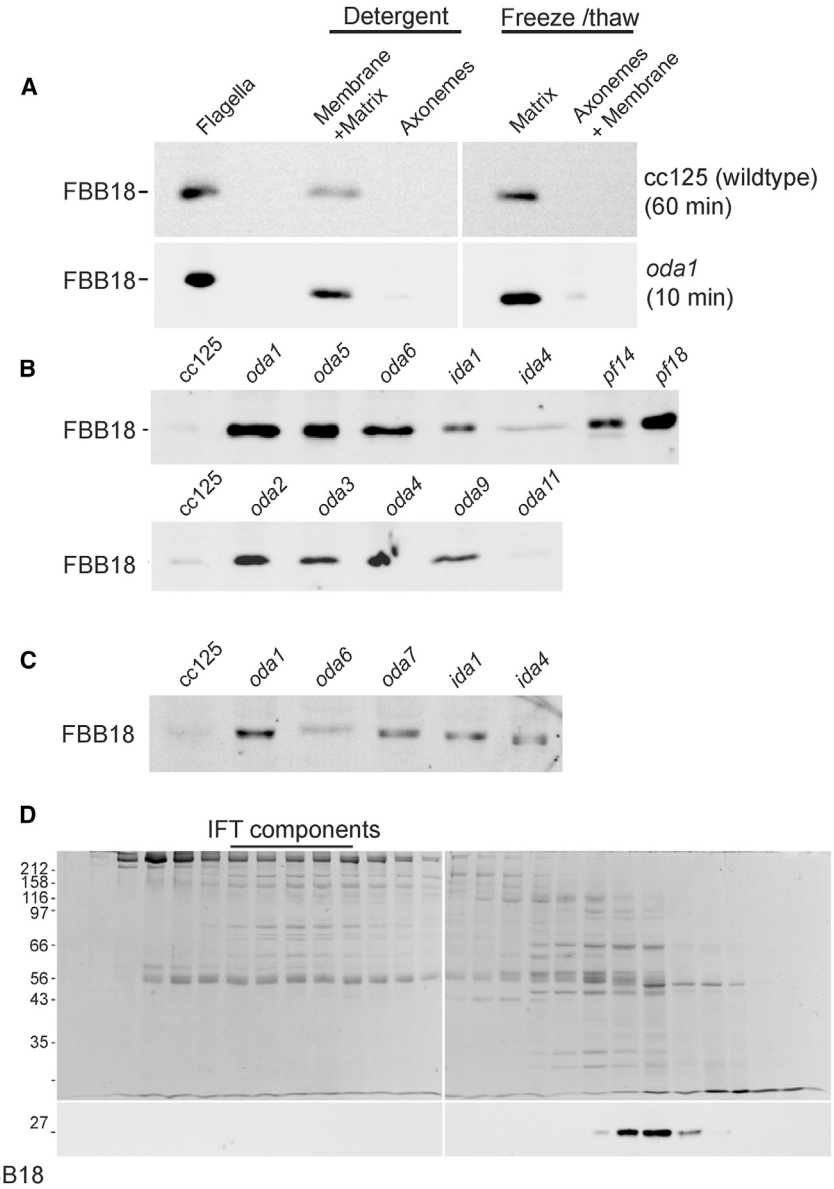

Figure 4. Analysis C21orf59/FBB18 in *C. reinhardtii*

(A) Flagella from wild-type and *oda1* mutant *Chlamydomonas* strains were extracted by detergent or freeze-thaw methods. FBB18 is found exclusively within the flagellar matrix in both strains. Note that blot exposure time was significantly longer for the wild-type strain.

(B) Probing flagella extracts from wild-type (cc125) and *Chlamydomonas* mutant strains with an FBB18 antibody reveals that flagella protein levels are significantly enhanced in cilia mutants with severe motility defects but not in *oda11*, which retains most of the outer arm and exhibits close to wild-type ciliary motility.

(C) FBB18 immunoblot of wild-type (cc125) and cilia mutant cell bodies shows increased FBB18 protein abundance in mutants with impaired cilia motility.

(D) Fractionation of *Chlamydomonas* flagella matrix extract in a Superose 6 gel filtration column. FBB18 migrates in a single peak distinct from core IFT complex proteins.

(Figures 1I and 6B), suggesting a different role for this protein in ciliary function. Recent studies in *C. reinhardtii* have identified the *CCDC65* ortholog *FAP250* (Cre13.g607750.t1.2)[55] as a subunit of the nexin-dynein regulatory complex.[17,56] The gene encoding FAP250 maps to the right arm of linkage group XIV (chromosome 13), in the vicinity of the *ida6* mutation (Figure 6G). *ida6* fails to assemble a single-headed, inner arm dynein and displays a slow swimming motility defect,[54] but it is not linked to any of the genes encoding DHC subunits.[57,58] To determine whether *ida6* might be a mutation in an accessory protein required for dynein assembly and motility, we transformed *ida6* with an ~9.5 kb genomic subclone containing *FAP250* and tested transformants for rescue of the slow-swimming phenotype. The observed restoration of forward swimming velocity (Figure 6H) and direct sequencing of *FAP250* demonstrated that *ida6* is a mutation that alters the stop codon of *FAP250/CCDC65* and thus adds 106 amino acids to the C terminus of the protein (Figure S11). To assess whether *ida6* also affects assembly of the N-DRC, we analyzed isolated axonemes by thin-section electron microscopy and computer image averaging.[37] Longitudinal views of the 96 nm axoneme repeats of WT, *pf3* (a previously characterized DRC mutant), *ida6*, and *IDA6* rescued (G11) strains revealed defects in the assembly of both the inner dynein arms and the N-DRC in *ida6* (Figure 6I). These defects were not observed in the rescued *ida6::IDA6* strain (Figure 6I), demonstrating that the structural defect was specific to the *FAP250* mutation. Immunoblotting revealed that both FAP250 and tektin were missing or reduced in isolated *ida6* axonemes (Figure 6J), indicating that the additional amino acids in *ida6* inhibited assembly of both FAP250 and tektin. As expected, both proteins were restored in axonemes from the rescued *ida6::IDA6* strain (Figure 6J). These data, together with the predicted size of the FAP250 polypeptide, strongly suggest that FAP250 corresponds to the DRC2 subunit of N-DRC and that DRC2/FAP250/CCDC65 plays a critical role in the assembly of the N-DRC.

Discussion

Although the structure of cilia and flagella has been studied for decades, proteomic analysis has only recently

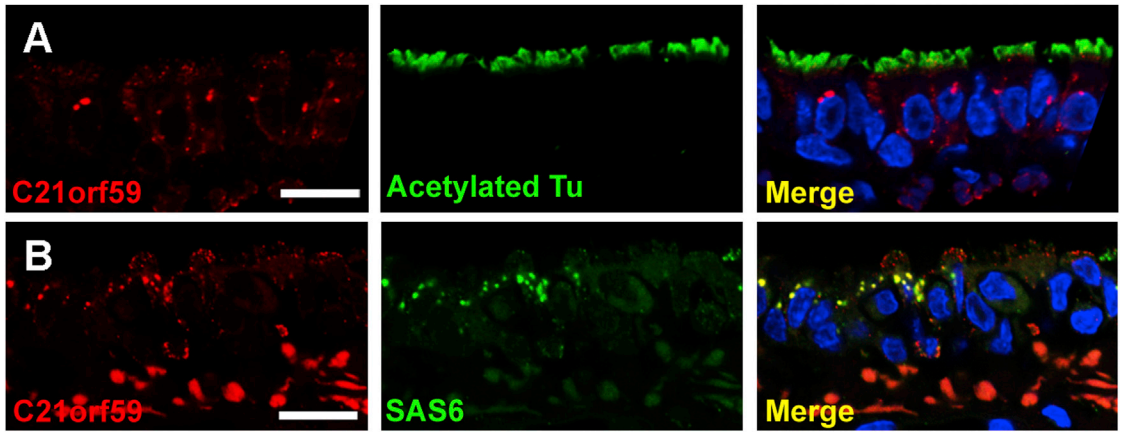

Figure 5. Cellular Localization of C21orf59 Protein
(A) C21orf59 immunostaining in rat trachea ciliated epithelial cells reveals predominant cytoplasmic localization in perinuclear puncta.
(B) C21orf59 colocalizes with SAS6 in cytoplasmic puncta in rat trachea ciliated epithelial cells.
Scale bars represent QA.

revealed the complexity of these organelles and their component protein subunits.[41,45,47,49] Our screen of cilia proteome candidate genes identified two genes, *C21orf59/FBB18* and *CCDC65/FAP250*, that are mutated in PCD and that act via distinct mechanisms to control cilia motility.

We found that both *c21orf59* zebrafish knockdown and *C21orf59* mutations in individuals with PCD resulted in complete cilia paralysis and the loss of both outer and inner dynein arms. Failure of the *C21orf59* nonsense mutant mRNA to rescue cilia motility in zebrafish was linked to a loss of stable protein levels, suggesting that human phenotypes might be due to the complete absence of C21orf59 protein, leading to failed ODA and DNALI1 related IDA assembly. Partial loss of rescuing activity by the c.422A>G (p.Asp141Gly) *C21orf59* mutant mRNA suggests that this allele could represent a hypomorphic mutation. Although the affected individuals harboring this mutation were heterozygous at the *C21orf59* locus, it remains possible that a hypomorphic mutation in *C21orf59* inherited with mutation(s) in other genes associated with dynein function or assembly could contribute to digenic or oligogenic transmission of PCD. Evidence for digenic inheritance in short-rib polydactyly syndrome type Majewski, a ciliopathy linked to paired heterozygous mutations in *NEK1* and *DYNC2H1,* has been reported.[59]

The stepwise sequence of cytoplasmic dynein arm assembly, transport, and axonemal docking has been well characterized in *Chlamydomonas reinhardtii* flagellar mutants. The mutated genes encode dynein motor subunits, axonemal docking complexes, and nonaxonemal dynein arm assembly and transport factors.[11,60,61] The C21orf59/FBB18 accumulation we observed at the basal body suggests a role in cytoplasmic dynein assembly or transport into the axoneme. However, the behavior of C21orf59/FBB18 appears to be unique relative to known ODA assembly proteins in that C21orf59/FBB18 accumulates dramatically in the matrix fraction of mutant axonemes that exhibit reduced motility. C21orf59/FBB18 is not strongly associated with the IFT particle in fractionated axonemes, suggesting that it might act as an adaptor protein for ODA and IDA transport. An increased abundance of flagellar C21orf59/FBB18 in axonemes correlated with increased protein levels in cell bodies as well, indicating that C21orf59/FBB18 is either stabilized or induced in response to flagellar immotility. Elevated cell body and axonemal C21orf59/FBB18 in flagellar mutants suggests that cells can detect impaired cilia motility and initiate molecular responses to compensate for motility defects. Mammalian multiciliated cells are known to modulate dynein arm activity in response to increased fluid viscosity,[62,63] indicating that cells monitor cilia movement and detect resistance to cilia beating. Intriguingly, a cellular abundance of *Chlamydomonas* Lis1 protein, a dynein regulatory factor that controls microtubule binding affinity, is enhanced in response to both genetic and environmental disruption of axonemal beating.[64] It could be that the abundance of C21orf59/FBB18 in cilia and flagella is differentially regulated in response to flagellar motility and that this protein might enhance ODA stability in "high-load" environments.

Our functional analysis of *CCDC65/FAP250/DRC2* revealed that this gene encodes a protein that is required for proper cilia motility. In contrast to *C21orf59*, *CCDC65* is not required for ODA structure and instead plays an essential role in regulating dynein activity. *CCDC65* is the vertebrate ortholog of *Chlamydomonas FAP250*, which encodes a protein recently identified as the DRC2 subunit of the N-DRC.[17,56] The N-DRC is a 12 subunit protein complex positioned on axonemes adjacent to inner dynein arms.[17,56] The N-DRC mediates both outer doublet alignment and the control of dynein activity in response to signals from radial spokes and the central pair apparatus.[13,17,65,66] Structural analysis of the N-DRC suggests that CCDC65/FAP250/DRC2, together with DRC1, forms the "base plate" of N-DRC, which makes

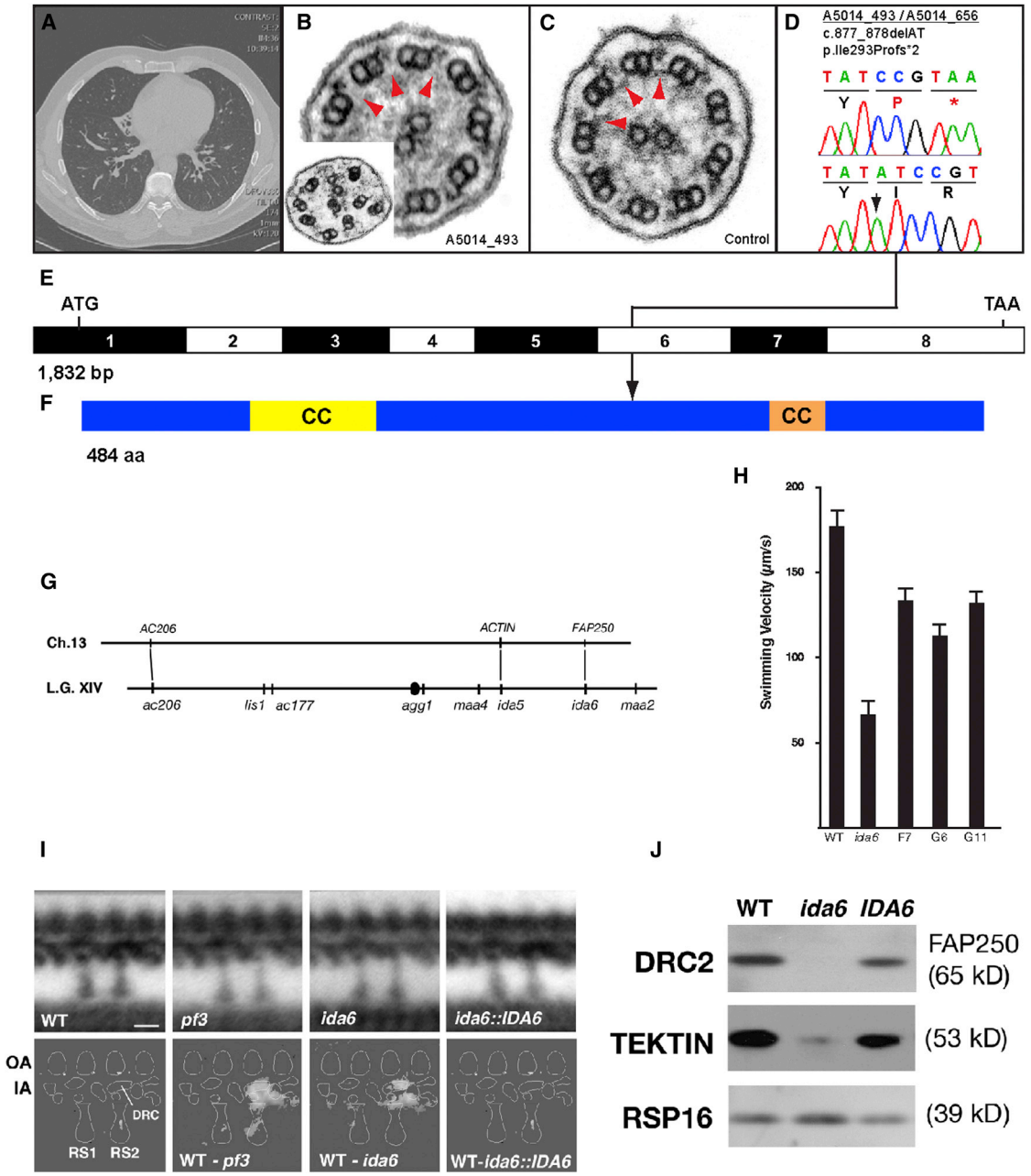

Figure 6. Identification of Recessive Mutations in *CCDC65* in Two Families with Primary Ciliary Dyskinesia and Identification of *FAP250/CCDC65* as the Causative Gene in the *ida6* Mutant

(A) Chest CT scan of individual A5014_493-21 showing volume loss and bronchiectasis in the right middle lobe and bronchiectasis in both lower lobes.

(B) TEM of individual A5014_493-21 cilia showing normal dynein arms and central pairs. Note that upon close examination, N-DRC links are missing (red arrowheads). Microtubule disorganization (B, inset) was observed in 5%–15% of PCD individual cilia sections.

(C) Control cilia TEM showing normal dynein inner arms and nexin links (red arrowheads).

(D) A homozygous truncating *CCDC65* mutation detected in two independent families with PCD. Family number (underlined), mutation (arrowhead), and predicted translational changes are indicated. Sequence trace is shown for mutation above normal control. For the mutations detected, arrows indicate positions in relation to exons.

(E) Exon structure of human *CCDC65* cDNA. Positions of start codon (ATG) and of stop codon (TAA) are indicated.

(F) Domain structure of the CCDC65 protein indicating two coiled-coil (CC) domains and position of truncating stop codon mutation.

(G–J) The *C. reinhardtii IDA6* gene encodes FAP250/DRC2/CCDC65.

(G) *FAP250* maps near the *ACTIN* gene on the right arm of *C. reinhardtii* Linkage Group XIV (chromosome 13), in the vicinity of the *ida6* mutation. *AC206* and *ACTIN* have been linked to the *ac206* and *ida5* mutations on the left and right arms of Linkage Group XIV, respectively (bottom line). *ida6* is an inner arm motility mutation located ~6 cM from *ida5*[54] and the *FAP250* gene is located ~6.1 Mb away from the *ACTIN* gene.

(legend continued on next page)

extensive connections with the outer doublet microtubules, radial spokes, and inner dynein arms.[13,17] Interestingly, the loss of CCDC65/FAP250 in the *Chlamydomonas ida6* mutant is also associated with a reduction of the protein Tektin in axonemes.[67] Tektin forms rod-like structures that have been proposed to stabilize microtubules and participate in the longitudinal spacing of axonemal components such as inner dynein arms and radial spokes.[68] The integrity of the 9+2 axoneme did not appear to be significantly affected in the *Chlamydomonas ida6* mutant but we did observe axonemal microtubular disorganization (MTD) in a subset of cilia sections from affected individuals bearing a mutation in *CCDC65*. MTD has been reported in other N-DRC mutants and in radial spokehead mutants,[69,70] suggesting that this defect might arise from loss of the putative radial spoke attachment site in *CCDC65* mutant axonemes. No clear evidence for MTD was observed in the *Chlamydomonas ida6* mutant, however. This and the low penetrance of MTD in *CCDC65* mutant axonemes suggests that MTD might occur only after prolonged cilia beating and that it might represent a terminal breakdown of cilia structure.

The third gene we identified in our zebrafish screen, *c15orf26*, was not mutated in our PCD cohort. However, a locus containing *C15orf26* (RefSeq accession number NM_173528.2) on chromosome 15 has previously been associated with PCD.[71] Cilia immotility in these individuals was associated with a lack of outer dynein arms, similar to the *c15orf26* knockdown phenotype in zebrafish. Although coding mutations in *C15orf26* were not found, mutations affecting mRNA splicing or transcriptional regulation were not ruled out. Further analysis of *C15orf26* expression in these individuals could therefore be informative.

Supplemental Data

Supplemental Data include Supplemental Acknowledgments, 11 figures, four tables, and nine movies and can be found with this article online at http://www.cell.com/AJHG/.

Acknowledgments

We are grateful to all PCD subjects and family members for their participation and thank the US PCD Foundation and to the investigators and the coordinators of the "Genetic Disorders of Mucociliary Clearance Consortium." We are also grateful to the funding agencies that supported this work; these include the National Institutes of Health, the Howard Hughes Medical Institute, the Deutsche Forschungsgemeinschaft, the IZKF Muenster, and the European Community's Seventh Framework Programme. Detailed acknowledgements can be found in the Supplemental Data.

Received: June 17, 2013
Revised: July 24, 2013
Accepted: August 28, 2013
Published: October 3, 2013

Web Resources

The URLs for data presented herein are as follows:

Chlamydomonas Resource Center, http://chlamycollection.org/
Online Mendelian Inheritance in Man (OMIM), http://www.omim.org/
RefSeq, http://www.ncbi.nlm.nih.gov/RefSeq
ZFIN, http://zfin.org

References

1. Veland, I.R., Awan, A., Pedersen, L.B., Yoder, B.K., and Christensen, S.T. (2009). Primary cilia and signaling pathways in mammalian development, health and disease. Nephron, Physiol. *111*, 39–53.
2. Fisch, C., and Dupuis-Williams, P. (2011). Ultrastructure of cilia and flagella - back to the future!. Biol. Cell *103*, 249–270.
3. Ibañez-Tallon, I., Heintz, N., and Omran, H. (2003). To beat or not to beat: roles of cilia in development and disease. Hum. Mol. Genet. *12*(Spec No 1), R27–R35.
4. Waters, A.M., and Beales, P.L. (2011). Ciliopathies: an expanding disease spectrum. Pediatr. Nephrol. *26*, 1039–1056.
5. Arts, H.H., Bongers, E.M., Mans, D.A., van Beersum, S.E., Oud, M.M., Bolat, E., Spruijt, L., Cornelissen, E.A., Schuurs-Hoeijmakers, J.H., de Leeuw, N., et al. (2011). C14ORF179 encoding IFT43 is mutated in Sensenbrenner syndrome. J. Med. Genet. *48*, 390–395.
6. Walczak-Sztulpa, J., Eggenschwiler, J., Osborn, D., Brown, D.A., Emma, F., Klingenberg, C., Hennekam, R.C., Torre, G., Garshasbi, M., Tzschach, A., et al. (2010). Cranioectodermal dysplasia, Sensenbrenner syndrome, is a ciliopathy caused by mutations in the IFT122 gene. Am. J. Hum. Genet. *86*, 949–956.

(H) The *ida6* motility mutant was transformed with an ~9.5 kb genomic subclone encoding FAP250, and transformants were screened for improved motility by phase-contrast microscopy. The forward swimming velocities of three rescued strains are shown here relative to wild-type and *ida6*.
(I) Longitudinal views of the 96 nm repeat of axonemes from WT, *pf3*, *ida6*, and an *IDA6* rescued strain (G11) were computer averaged and then compared to identify regions of statistically significant differences. The top row shows the average of the 96 nm repeat for each strain, whereas the bottom row shows the difference plots between the wild-type and each sample. A schematic diagram of the densities observed in each repeat is labeled on the bottom left. The crescent-shaped region associated with the dynein regulatory complex (DRC) is located above radial spoke 2 (RS2), between the outer arms (OA) and inner arms (IA). Both *pf3* and *ida6* are associated with significant defects in the assembly of the DRC and closely associated inner arm dyneins (see difference plots). These defects are not observed in the rescued *ida6::IDA6* strain. The number of axonemes and 96 nm repeats analyzed for each strain are as follows: wild-type (9 axonemes, 62 repeats), *pf3* (7 axonemes, 63 repeats), *ida6* (4 axonemes, 35 repeats), and *ida6::IDA6* (7 axonemes, 60 repeats).
(J) Axonemes from WT, *ida6*, and a rescued *IDA6* strain were analyzed on an immunoblot probed with antibodies against several flagellar proteins. Both FAP250 (DRC2) and tektin are missing or reduced in *ida6* and restored to near wild-type levels in the rescued *IDA6* strain. The RSP16 subunit of the radial spokes serves as a loading control.
Scale bars in (A) and (B) represent 20 μm.

7. Bredrup, C., Saunier, S., Oud, M.M., Fiskerstrand, T., Hoischen, A., Brackman, D., Leh, S.M., Midtbø, M., Filhol, E., Bole-Feysot, C., et al. (2011). Ciliopathies with skeletal anomalies and renal insufficiency due to mutations in the IFT-A gene WDR19. Am. J. Hum. Genet. *89*, 634–643.
8. Zariwala, M.A., Omran, H., and Ferkol, T.W. (2011). The emerging genetics of primary ciliary dyskinesia. Proc. Am. Thorac. Soc. *8*, 430–433.
9. Guichard, C., Harricane, M.C., Lafitte, J.J., Godard, P., Zaegel, M., Tack, V., Lalau, G., and Bouvagnet, P. (2001). Axonemal dynein intermediate-chain gene (DNAI1) mutations result in situs inversus and primary ciliary dyskinesia (Kartagener syndrome). Am. J. Hum. Genet. *68*, 1030–1035.
10. Olbrich, H., Häffner, K., Kispert, A., Völkel, A., Volz, A., Sasmaz, G., Reinhardt, R., Hennig, S., Lehrach, H., Konietzko, N., et al. (2002). Mutations in DNAH5 cause primary ciliary dyskinesia and randomization of left-right asymmetry. Nat. Genet. *30*, 143–144.
11. Omran, H., Kobayashi, D., Olbrich, H., Tsukahara, T., Loges, N.T., Hagiwara, H., Zhang, Q., Leblond, G., O'Toole, E., Hara, C., et al. (2008). Ktu/PF13 is required for cytoplasmic pre-assembly of axonemal dyneins. Nature *456*, 611–616.
12. Panizzi, J.R., Becker-Heck, A., Castleman, V.H., Al-Mutairi, D.A., Liu, Y., Loges, N.T., Pathak, N., Austin-Tse, C., Sheridan, E., Schmidts, M., et al. (2012). CCDC103 mutations cause primary ciliary dyskinesia by disrupting assembly of ciliary dynein arms. Nat. Genet. *44*, 714–719.
13. Heuser, T., Raytchev, M., Krell, J., Porter, M.E., and Nicastro, D. (2009). The dynein regulatory complex is the nexin link and a major regulatory node in cilia and flagella. J. Cell Biol. *187*, 921–933.
14. Wirschell, M., Olbrich, H., Werner, C., Tritschler, D., Bower, R., Sale, W.S., Loges, N.T., Pennekamp, P., Lindberg, S., Stenram, U., et al. (2013). The nexin-dynein regulatory complex subunit DRC1 is essential for motile cilia function in algae and humans. Nat. Genet. *45*, 262–268.
15. Williams, B.D., Velleca, M.A., Curry, A.M., and Rosenbaum, J.L. (1989). Molecular cloning and sequence analysis of the *Chlamydomonas* gene coding for radial spoke protein 3: flagellar mutation pf-14 is an ochre allele. J. Cell Biol. *109*, 235–245.
16. Castleman, V.H., Romio, L., Chodhari, R., Hirst, R.A., de Castro, S.C.P., Parker, K.A., Ybot-Gonzalez, P., Emes, R.D., Wilson, S.W., Wallis, C., et al. (2009). Mutations in radial spoke head protein genes RSPH9 and RSPH4A cause primary ciliary dyskinesia with central-microtubular-pair abnormalities. Am. J. Hum. Genet. *84*, 197–209.
17. Bower, R., Tritschler, D., Vanderwaal, K., Perrone, C.A., Mueller, J., Fox, L., Sale, W.S., and Porter, M.E. (2013). The N-DRC forms a conserved biochemical complex that maintains outer doublet alignment and limits microtubule sliding in motile axonemes. Mol. Biol. Cell *24*, 1134–1152.
18. Gherman, A., Davis, E.E., and Katsanis, N. (2006). The ciliary proteome database: an integrated community resource for the genetic and functional dissection of cilia. Nat. Genet. *38*, 961–962.
19. Westerfield, M. (2007). The Zebrafish Book: A Guide for the Laboratory Use of Zebrafish (*Danio rerio*) (Eugene, OR: University of Oregon Press).
20. Suster, M.L., Kikuta, H., Urasaki, A., Asakawa, K., and Kawakami, K. (2009). Transgenesis in zebrafish with the tol2 transposon system. Methods Mol. Biol. *561*, 41–63.
21. Kwan, K.M., Fujimoto, E., Grabher, C., Mangum, B.D., Hardy, M.E., Campbell, D.S., Parant, J.M., Yost, H.J., Kanki, J.P., and Chien, C.B. (2007). The Tol2kit: a multisite gateway-based construction kit for Tol2 transposon transgenesis constructs. Dev. Dyn. *236*, 3088–3099.
22. Thisse, B., Heyer, V., Lux, A., Alunni, V., Degrave, A., Seiliez, I., Kirchner, J., Parkhill, J.P., and Thisse, C. (2004). Spatial and temporal expression of the zebrafish genome by large-scale in situ hybridization screening. Methods Cell Biol. *77*, 505–519.
23. Hellman, N.E., Liu, Y., Merkel, E., Austin, C., Le Corre, S., Beier, D.R., Sun, Z., Sharma, N., Yoder, B.K., and Drummond, I.A. (2010). The zebrafish foxj1a transcription factor regulates cilia function in response to injury and epithelial stretch. Proc. Natl. Acad. Sci. USA *107*, 18499–18504.
24. Panizzi, J.R., Jessen, J.R., Drummond, I.A., and Solnica-Krezel, L. (2007). New functions for a vertebrate Rho guanine nucleotide exchange factor in ciliated epithelia. Development *134*, 921–931.
25. Pathak, N., Austin, C.A., and Drummond, I.A. (2011). Tubulin tyrosine ligase-like genes ttll3 and ttll6 maintain zebrafish cilia structure and motility. J. Biol. Chem. *286*, 11685–11695.
26. Rashid, S., Breckle, R., Hupe, M., Geisler, S., Doerwald, N., and Neesen, J. (2006). The murine *Dnali1* gene encodes a flagellar protein that interacts with the cytoplasmic dynein heavy chain 1. Mol. Reprod. Dev. *73*, 784–794.
27. Drummond, I.A., Majumdar, A., Hentschel, H., Elger, M., Solnica-Krezel, L., Schier, A.F., Neuhauss, S.C., Stemple, D.L., Zwartkruis, F., Rangini, Z., et al. (1998). Early development of the zebrafish pronephros and analysis of mutations affecting pronephric function. Development *125*, 4655–4667.
28. Loges, N.T., Olbrich, H., Becker-Heck, A., Häffner, K., Heer, A., Reinhard, C., Schmidts, M., Kispert, A., Zariwala, M.A., Leigh, M.W., et al. (2009). Deletions and point mutations of LRRC50 cause primary ciliary dyskinesia due to dynein arm defects. Am. J. Hum. Genet. *85*, 883–889.
29. Rompolas, P., Patel-King, R.S., and King, S.M. (2010). An outer arm Dynein conformational switch is required for metachronal synchrony of motile cilia in planaria. Mol. Biol. Cell *21*, 3669–3679.
30. Costa, G.L., Bauer, J.C., McGowan, B., Angert, M., and Weiner, M.P. (1996). Site-directed mutagenesis using a rapid PCR-based method. Methods Mol. Biol. *57*, 239–248.
31. Timmons, L., and Fire, A. (1998). Specific interference by ingested dsRNA. Nature *395*, 854.
32. Newmark, P.A., Reddien, P.W., Cebrià, F., and Sánchez Alvarado, A. (2003). Ingestion of bacterially expressed double-stranded RNA inhibits gene expression in planarians. Proc. Natl. Acad. Sci. USA *100*(*Suppl 1*), 11861–11865.
33. Rompolas, P., Patel-King, R.S., and King, S.M. (2009). *Schmidtea mediterranea*: a model system for analysis of motile cilia. Methods Cell Biol. *93*, 81–98.
34. Witman, G.B., Carlson, K., Berliner, J., and Rosenbaum, J.L. (1972). *Chlamydomonas* flagella. I. Isolation and electrophoretic analysis of microtubules, matrix, membranes, and mastigonemes. J. Cell Biol. *54*, 507–539.
35. Rompolas, P., Pedersen, L.B., Patel-King, R.S., and King, S.M. (2007). *Chlamydomonas* FAP133 is a dynein intermediate chain associated with the retrograde intraflagellar transport motor. J. Cell Sci. *120*, 3653–3665.
36. Sizova, I., Fuhrmann, M., and Hegemann, P. (2001). A *Streptomyces rimosus aphVIII* gene coding for a new type

phosphotransferase provides stable antibiotic resistance to *Chlamydomonas reinhardtii*. Gene *277*, 221–229.
37. O'Toole, E., Mastronarde, D., McIntosh, J.R., and Porter, M.E. (1995). Computer-assisted analysis of flagellar structure. Methods Cell Biol. *47*, 183–191.
38. Leigh, M.W., Pittman, J.E., Carson, J.L., Ferkol, T.W., Dell, S.D., Davis, S.D., Knowles, M.R., and Zariwala, M.A. (2009). Clinical and genetic aspects of primary ciliary dyskinesia/Kartagener syndrome. Genet. Med. *11*, 473–487.
39. Halbritter, J., Diaz, K., Chaki, M., Porath, J.D., Tarrier, B., Fu, C., Innis, J.L., Allen, S.J., Lyons, R.H., Stefanidis, C.J., et al. (2012). High-throughput mutation analysis in patients with a nephronophthisis-associated ciliopathy applying multiplexed barcoded array-based PCR amplification and next-generation sequencing. J. Med. Genet. *49*, 756–767.
40. Otto, E.A., Helou, J., Allen, S.J., O'Toole, J.F., Wise, E.L., Ashraf, S., Attanasio, M., Zhou, W., Wolf, M.T.F., and Hildebrandt, F. (2008). Mutation analysis in nephronophthisis using a combined approach of homozygosity mapping, CEL I endonuclease cleavage, and direct sequencing. Hum. Mutat. *29*, 418–426.
41. Avidor-Reiss, T., Maer, A.M., Koundakjian, E., Polyanovsky, A., Keil, T., Subramaniam, S., and Zuker, C.S. (2004). Decoding cilia function: defining specialized genes required for compartmentalized cilia biogenesis. Cell *117*, 527–539.
42. Broadhead, R., Dawe, H.R., Farr, H., Griffiths, S., Hart, S.R., Portman, N., Shaw, M.K., Ginger, M.L., Gaskell, S.J., McKean, P.G., and Gull, K. (2006). Flagellar motility is required for the viability of the bloodstream trypanosome. Nature *440*, 224–227.
43. Stolc, V., Samanta, M.P., Tongprasit, W., and Marshall, W.F. (2005). Genome-wide transcriptional analysis of flagellar regeneration in *Chlamydomonas reinhardtii* identifies orthologs of ciliary disease genes. Proc. Natl. Acad. Sci. USA *102*, 3703–3707.
44. Ostrowski, L.E., Blackburn, K., Radde, K.M., Moyer, M.B., Schlatzer, D.M., Moseley, A., and Boucher, R.C. (2002). A proteomic analysis of human cilia: identification of novel components. Mol. Cell. Proteomics *1*, 451–465.
45. Efimenko, E., Bubb, K., Mak, H.Y., Holzman, T., Leroux, M.R., Ruvkun, G., Thomas, J.H., and Swoboda, P. (2005). Analysis of *xbx* genes in *C. elegans*. Development *132*, 1923–1934.
46. Liu, Q., Tan, G., Levenkova, N., Li, T., Pugh, E.N., Jr., Rux, J.J., Speicher, D.W., and Pierce, E.A. (2007). The proteome of the mouse photoreceptor sensory cilium complex. Mol. Cell. Proteomics *6*, 1299–1317.
47. Li, J.B., Gerdes, J.M., Haycraft, C.J., Fan, Y., Teslovich, T.M., May-Simera, H., Li, H., Blacque, O.E., Li, L., Leitch, C.C., et al. (2004). Comparative genomics identifies a flagellar and basal body proteome that includes the BBS5 human disease gene. Cell *117*, 541–552.
48. Andersen, J.S., Wilkinson, C.J., Mayor, T., Mortensen, P., Nigg, E.A., and Mann, M. (2003). Proteomic characterization of the human centrosome by protein correlation profiling. Nature *426*, 570–574.
49. Pazour, G.J., Agrin, N., Leszyk, J., and Witman, G.B. (2005). Proteomic analysis of a eukaryotic cilium. J. Cell Biol. *170*, 103–113.
50. Keller, L.C., Romijn, E.P., Zamora, I., Yates, J.R., 3rd, and Marshall, W.F. (2005). Proteomic analysis of isolated chlamydomonas centrioles reveals orthologs of ciliary-disease genes. Curr. Biol. *15*, 1090–1098.
51. Yu, X., Ng, C.P., Habacher, H., and Roy, S. (2008). Foxj1 transcription factors are master regulators of the motile ciliogenic program. Nat. Genet. *40*, 1445–1453.
52. Robb, S.M., Ross, E., and Sánchez Alvarado, A. (2008). SmedGD: the *Schmidtea mediterranea* genome database. Nucleic Acids Res. *36*(Database issue), D599–D606.
53. Noone, P.G., Leigh, M.W., Sannuti, A., Minnix, S.L., Carson, J.L., Hazucha, M., Zariwala, M.A., and Knowles, M.R. (2004). Primary ciliary dyskinesia: diagnostic and phenotypic features. Am. J. Respir. Crit. Care Med. *169*, 459–467.
54. Kato, T., Kagami, O., Yagi, T., and Kamiya, R. (1993). Isolation of two species of *Chlamydomonas reinhardtii* flagellar mutants, ida5 and ida6, that lack a newly identified heavy chain of the inner dynein arm. Cell Struct. Funct. *18*, 371–377.
55. Goodstein, D.M., Shu, S., Howson, R., Neupane, R., Hayes, R.D., Fazo, J., Mitros, T., Dirks, W., Hellsten, U., Putnam, N., and Rokhsar, D.S. (2012). Phytozome: a comparative platform for green plant genomics. Nucleic Acids Res. *40*(Database issue), D1178–D1186.
56. Lin, J., Tritschler, D., Song, K., Barber, C.F., Cobb, J.S., Porter, M.E., and Nicastro, D. (2011). Building blocks of the nexin-dynein regulatory complex in *Chlamydomonas* flagella. J. Biol. Chem. *286*, 29175–29191.
57. Porter, M.E., Knott, J.A., Myster, S.H., and Farlow, S.J. (1996). The dynein gene family in *Chlamydomonas reinhardtii*. Genetics *144*, 569–585.
58. Perrone, C.A., Yang, P., O'Toole, E., Sale, W.S., and Porter, M.E. (1998). The *Chlamydomonas* IDA7 locus encodes a 140-kDa dynein intermediate chain required to assemble the I1 inner arm complex. Mol. Biol. Cell *9*, 3351–3365.
59. Thiel, C., Kessler, K., Giessl, A., Dimmler, A., Shalev, S.A., von der Haar, S., Zenker, M., Zahnleiter, D., Stöss, H., Beinder, E., et al. (2011). NEK1 mutations cause short-rib polydactyly syndrome type majewski. Am. J. Hum. Genet. *88*, 106–114.
60. Ahmed, N.T., Gao, C., Lucker, B.F., Cole, D.G., and Mitchell, D.R. (2008). ODA16 aids axonemal outer row dynein assembly through an interaction with the intraflagellar transport machinery. J. Cell Biol. *183*, 313–322.
61. Fowkes, M.E., and Mitchell, D.R. (1998). The role of preassembled cytoplasmic complexes in assembly of flagellar dynein subunits. Mol. Biol. Cell *9*, 2337–2347.
62. Johnson, N.T., Villalón, M., Royce, F.H., Hard, R., and Verdugo, P. (1991). Autoregulation of beat frequency in respiratory ciliated cells. Demonstration by viscous loading. Am. Rev. Respir. Dis. *144*, 1091–1094.
63. Andrade, Y.N., Fernandes, J., Vázquez, E., Fernández-Fernández, J.M., Arniges, M., Sánchez, T.M., Villalón, M., and Valverde, M.A. (2005). TRPV4 channel is involved in the coupling of fluid viscosity changes to epithelial ciliary activity. J. Cell Biol. *168*, 869–874.
64. Rompolas, P., Patel-King, R.S., and King, S.M. (2012). Association of Lis1 with outer arm dynein is modulated in response to alterations in flagellar motility. Mol. Biol. Cell *23*, 3554–3565.
65. Piperno, G., Mead, K., and Shestak, W. (1992). The inner dynein arms I2 interact with a "dynein regulatory complex" in *Chlamydomonas* flagella. J. Cell Biol. *118*, 1455–1463.
66. Piperno, G., Mead, K., LeDizet, M., and Moscatelli, A. (1994). Mutations in the "dynein regulatory complex" alter the ATP-insensitive binding sites for inner arm dyneins in *Chlamydomonas* axonemes. J. Cell Biol. *125*, 1109–1117.

67. Yanagisawa, H.A., and Kamiya, R. (2004). A tektin homologue is decreased in *Chlamydomonas* mutants lacking an axonemal inner-arm dynein. Mol. Biol. Cell *15*, 2105–2115.
68. Amos, L.A. (2008). The tektin family of microtubule-stabilizing proteins. Genome Biol. *9*, 229.
69. Merveille, A.C., Davis, E.E., Becker-Heck, A., Legendre, M., Amirav, I., Bataille, G., Belmont, J., Beydon, N., Billen, F., Clément, A., et al. (2011). CCDC39 is required for assembly of inner dynein arms and the dynein regulatory complex and for normal ciliary motility in humans and dogs. Nat. Genet. *43*, 72–78.
70. Ziętkiewicz, E., Bukowy-Bieryłło, Z., Voelkel, K., Klimek, B., Dmeńska, H., Pogorzelski, A., Sulikowska-Rowińska, A., Rutkiewicz, E., and Witt, M. (2012). Mutations in radial spoke head genes and ultrastructural cilia defects in East-European cohort of primary ciliary dyskinesia patients. PLoS ONE *7*, e33667.
71. Geremek, M., Schoenmaker, F., Zietkiewicz, E., Pogorzelski, A., Diehl, S., Wijmenga, C., and Witt, M. (2008). Sequence analysis of 21 genes located in the Kartagener syndrome linkage region on chromosome 15q. Eur. J. Hum. Genet. *16*, 688–695.